

Chapter 1

INTRODUCTION

In this thesis the problems of surveying and processing magnetic data from areas contaminated by near surface, high intensity magnetic noise have been addressed. In particular, the study has concentrated upon a case study area where a known orebody existed in an environment characterized by the presence of near surface magnetic gravels giving rise to intense magnetic interference. The study area was the Elura Ag, Pb, Zn orebody located about 43 km NNW of Cobar in central New South Wales, Australia. A location map was provided in Figure 1.1. The survey area was gently undulating with a widespread cover of aeolian and alluvial magnetic gravels and mature palaeochannels where magnetite was concentrated.

1.1 State of the Art

One of the fundamental problems in using the magnetic method for deep source exploration in areas of near surface magnetic interference is to obtain results in which the noise is either eliminated or can be distinguished from the signal. The problem is very important in the determination of deep geological structures which are covered by a mask of weathered sediments. In the Australian environment, such sediments are frequently rich in magnetic iron minerals. Although efforts have been made in the past to recognize signal from noise, quantitative analysis of the noise has been severely limited by available

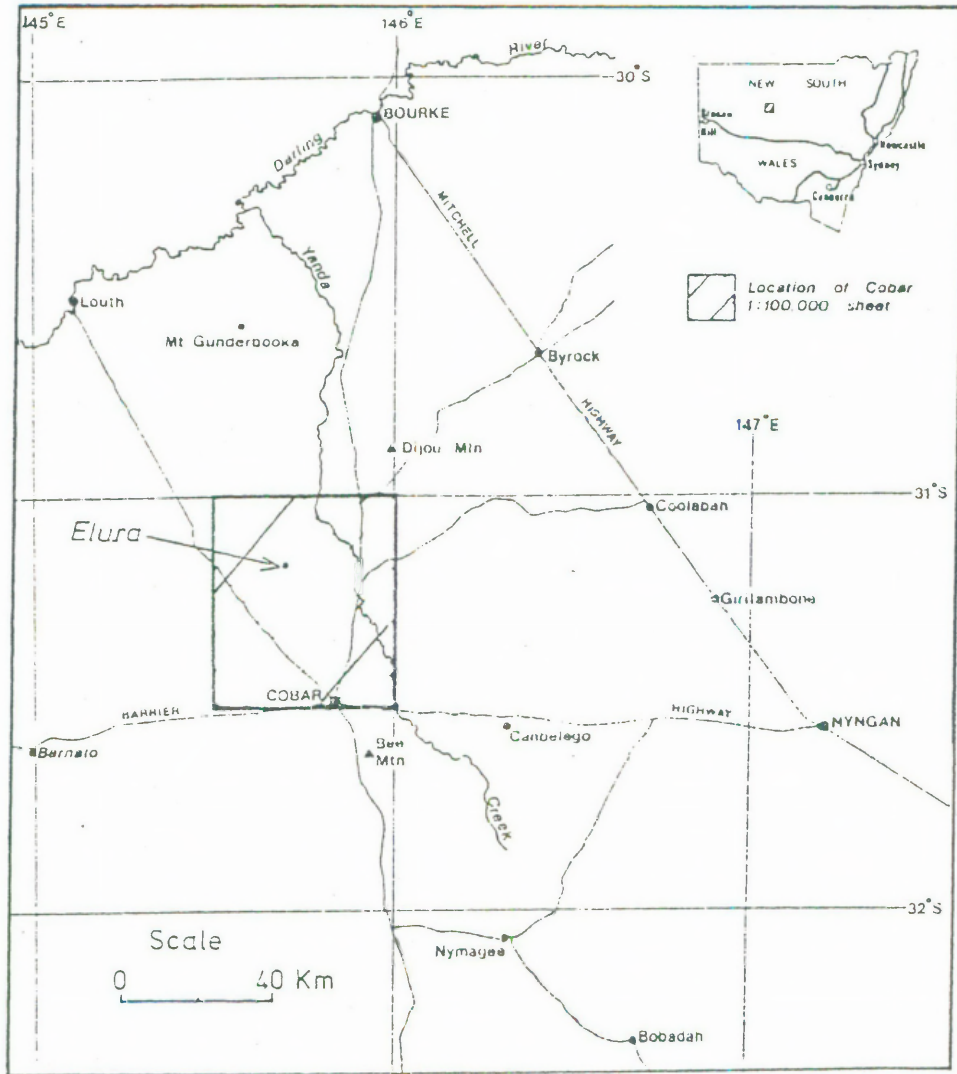


FIGURE 1.1: Location of the Elura area.

instrument technology and the logistics of adequately sampling the noise waveform. The present study was facilitated by the advent of new technology in magnetometer system design and hence for the first time adequate data was available for a quantitative study of signal and noise parameters.

A number of papers have been published concerning the separation of magnetic signal and noise but they have usually related to the special situation where the noise has been undersampled. In Chapter 5 a review of relevant filtering techniques was given.

The importance of the near surface magnetic noise problem in Australian mineral exploration was emphasized in 1978 at a symposium on 'Applied Magnetic Interpretation'. This symposium was sponsored and its proceedings published by the Australian Society of Exploration Geophysicists (Emerson, 1980). The discussion was mainly concentrated on the relationship between data sample interval and magnetometer sensor height so as to prevent aliasing. Prejudiced by the logistical problems of adequately sampling the noise spectrum at near ground level, the symposium favoured the use of airborne magnetics as a means of attenuating the interference from near surface noise sources. The underlying philosophy was based upon the fact that the near surface noise waveform would attenuate at a faster rate with sensor elevation than would the deep source signal.

Stanley (1979) proposed the alternative philosophy that provided the noise waveform was adequately sampled, then recording data close to the ground would maximize the deep signal amplitude. At the same time Stanley recognized that while the noise waveform would be amplified dramatically by this strategy, the amplified noise energy would almost entirely be confined to the high frequency end of the spectrum and should therefore be removable by appropriate filtering. With the development of a rapid sampling, automatic recording caesium magnetometer (Stanley 1975a, b, 1982) the logistics of magnetic field measurements at down to 0.2 m intervals was overcome. At this sample interval, traversing could be performed at up to seven km per hour.

1.2 Objectives of this study

The primary objectives of this study were to quantify the signal and noise waveform parameters, to quantify the signal to noise ratio that could be achieved from both airborne and ground level magnetic surveys in the presence of intense near surface magnetic noise and to investigate filtering operations that could be applied to airborne or ground level magnetic data.

The above objectives were seen as being relevant to many situations where a deep source anomaly of interest is to be measured in an environment where there is relatively intense near surface magnetic interference. While other such noise sources were considered, emphasis was placed upon a detailed case study of an area in which maghemitic gravels at or near the ground surface provide a very intense magnetic interference. Such situations occur frequently in mineralized environments within the Australian durrocrust.

In order to broaden the results from the specific case study area, calculations were made to determine the maximum depth and minimum tonnage of pyrrhotitic ore that could be expected to be located in the Cobar case study environment.

A final objectives of the study was to apply the optimized data processing procedure to the situation of detecting a theoretical orebody of defined parameters occurring beneath the extremely magnetized screen of a maghemitic palaeochannel.

1.3 The Elura Case Study

A great deal of the discussion about the problems of magnetic exploration in noisy environments which took place at the 1978 Symposium in Applied Magnetic Interpretation, was directed to the specific example of the Elura Ag, Pb, Zn orebody. This orebody had been recently discovered 1974 (Davis, 1980) and was the topic of intensive geophysical study. Interest in Elura was strong because it represented a geophysical target of moderate dimension in an environment that was very typical

of the Australian durocrust and which was particularly testing of geophysical techniques. Moreover, the orebody was available for study prior to the introduction of mine development equipments.

Chapter 2

THE ELURA CASE STUDY ENVIRONMENT

2.1 Introduction

Intermittent production of copper and gold from the Cobar field since its discovery in 1870 made this area the biggest source of copper in NSW and an important gold producer. Estimated ore reserves including past production totalled approximately 50 million tonnes.

Within the exploration rationale for the Cobar region was the geological premise that the mineralization was strata-bound. Previous mineral occurrences all lay along an arcuate belt trending generally north south. North of the known mineralization, deep soil cover and minimal exposure restricted exploration.

Davis (1980) reported that airborne magnetics was selected as the primary search tool because all known mineralization in the area was considered to have a magnetic signature. The first magnetic survey was flown in 1972 using a Geometrics G-803 proton magnetometer, flying at 90 metres with a line spacing of 300 metres.

Many anomalies were identified from the aeromagnetic data and these were systematically explored on the ground. Many of the anomalies were found to be associated with deep maghemitic channels and further exploration abandoned. The Elura anomaly displayed an amplitude of 30 nT. Geochemical sampling in 1973 revealed anomalous

Pb concentrations. Drilling in 1974 intersected gossan at 102 metres and sulphide at 133 metres.

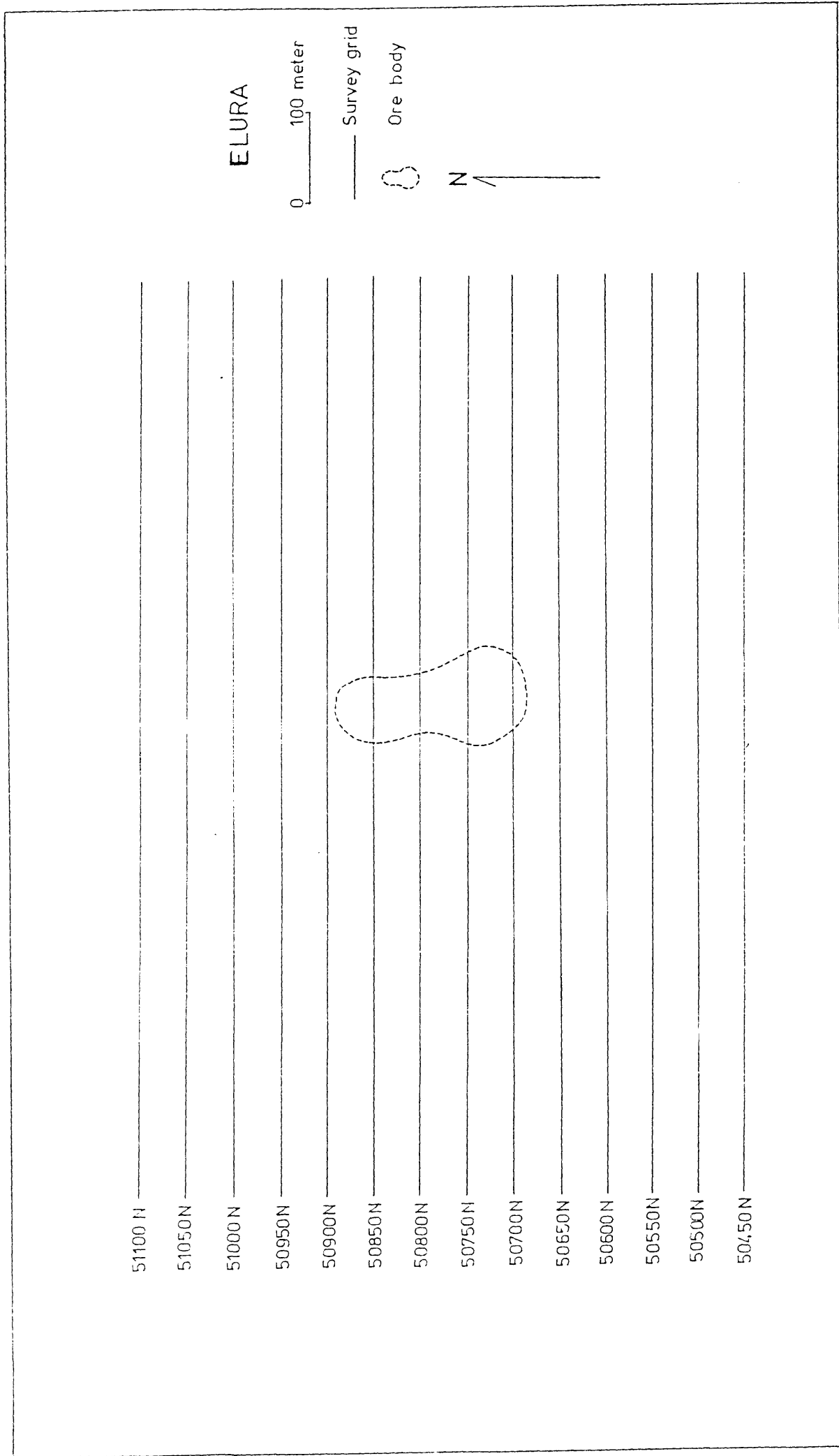
2.2 Local Geology

2.2.1 The Elura Orebody

Figure 2.1 is a survey grid which had been installed by the Electrolytic Zinc Company at the site of the known Zn-Pb-Ag orebody. Survey lines were oriented in the E-W direction. Each line is one kilometre long and 50 metres apart. The line numbers extend from 50450N south of the orebody to 51100N in the north. The fourteen lines cover an area of 650 x 1000 square metres with the orebody in the middle. The survey lines numbered 50850N to 50700N pass directly over the orebody. At the time of collecting data, the area had been disturbed by drill hole activities but plant installation had not begun.

The regional geology of the Cobar/Elura area is shown in Figure 2.2 (Adams and Schmidt, 1980). The rocks of the area have been mapped as two major rock units. They are the Girilambone Beds (basement rocks), and the Cobar Super-Group.

The basement rocks consist of the Ballast Beds and are the oldest rock unit in the area. The rocks are mainly sandstone, siltstone and shale, with minor chert and conglomerate (Baker, 1978). The Cobar Super-Group is separated from the basement rocks by an unconformity. The younger rock unit includes conglomerate, sandstone, siltstone, shale and quartzite. A granitic intrusion called the Tinderra Granite occurred between these two rock units. Detailed lithology and stratigraphy of the rock units can be found in Baker, Schmidt and Sherwin (1975), Brooke (1976), Pogson, Suppel, Gilligan, Scheibner, Baker, Sherwin, Brown, Felton and Fail (1976), Pogson and Felton (1978) and Baker (1978).



8.

FIGURE 2.1: The Elura survey grid showing the outline of the orebody at 100 m depth. Caesium magnetometer profiles covering this grid are contained in Appendix I.

6.

6.

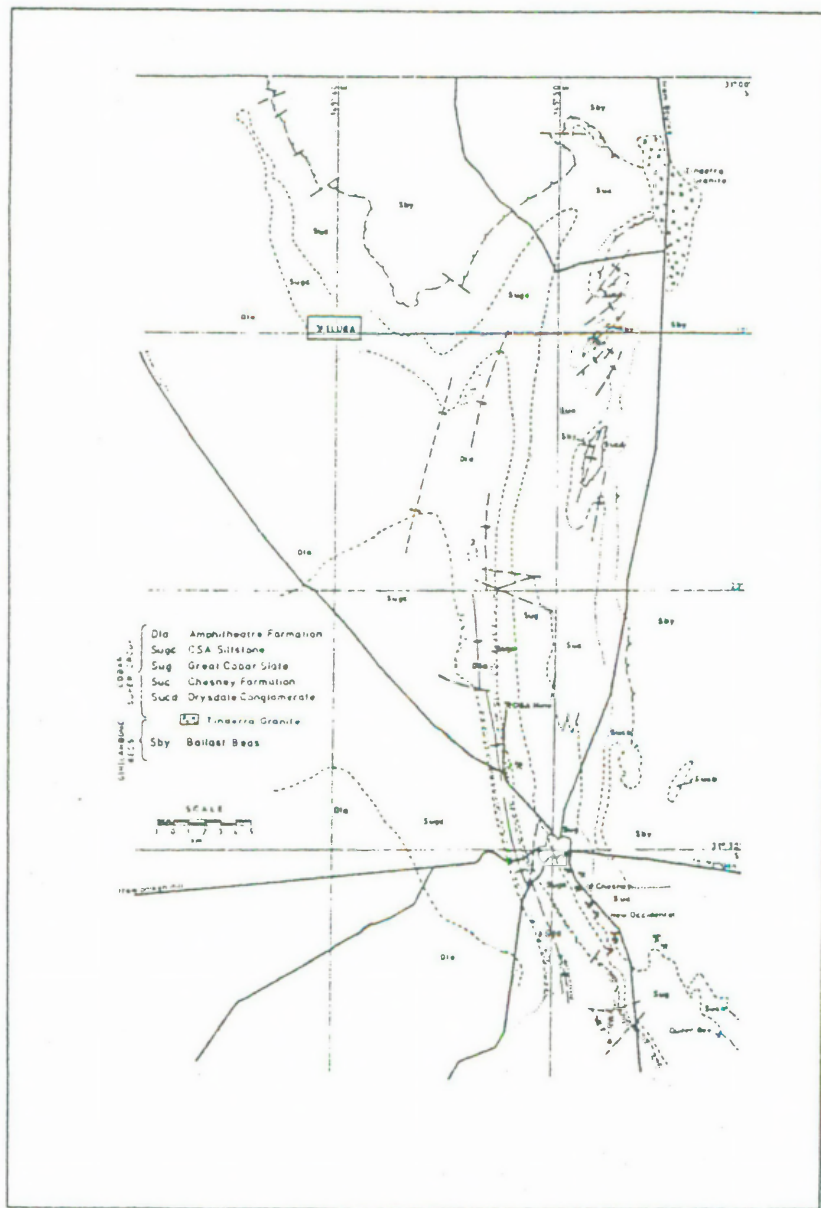


FIGURE 2.2: Regional geology of the Cobar area (taken from Adams and Schmidt, 1980).

Typical structures of the Ballast Beds are the well-developed cleavage, moderate to tight minor folds, and, in places, a crenulation cleavage. The folds range from centimetres to a few metres in wavelength (Baker, 1978).

Within the Cobar Super-Group, the structures are described by Brooke (1976) as broad folding compared with the tighter folding of the underlying rocks. The Cobar Super-Group forms the western limb of the fold structure - an anticline with strike 348° and dip $50 - 80^{\circ}$ W in the Cobar district. The anticline plunges 45° S. Some minor overturned folding is found, but easterly dips and facings are rarely seen. Other structures are also quoted from Brooke (1976) as follows :

A strong regional cleavage which is parallel to the axial plane of folding, strikes 355° and dip $45 - 85^{\circ}$ E. Movement has occurred in varying degrees sub-parallel to this cleavage, culminating in shears. Dominant stress relief has been east block-north movement along the shears, and there is little cross faulting.

For broad structures or tectonics of the area, tectonic models of the Cobar area were proposed suggesting a trough with subsequent deposition of the Cobar Super-Group (Kappelle, 1970 ; Baker et al., 1975; Pogson et al., 1976; Scheibner and Markham, 1976). The trough was in an extensional environment, so that its basin was formed as a fault bound trough (Baker et al., 1975; Pogson et al., 1976). Sangster (1979) proposed a growth fault or group of faults for a contact between the basement rock and the Cobar Super-Group, so that the trough formed in this part of the area. This reconstruction explains the sedimentation in the trough and the development of mineralization by exhalative deposit. The setting of the mineral deposits was proposed to be within three lines by Gilligan and Suppel (1978), but Sangster (1979) proposed four lines. Their deposits were: (i) in the C.S.A. siltstone Member (e.g. C.S.A., Elura, Mopone grid, and Spotted Leopard); (ii) in the Great Cobar Slate (Great Cobar, Dapville and Gladstone); (iii) at the contact between the Chesney Formation and Great Cobar Slate (New Cobar, Chesney, New Occidental, Tharsis, East

Cobar, Old Fort Brouke, Burrabingie, Wood Duck, Coronation, and Beechworth); (iv) at the contact between the Chesney Formation and the Drysdale conglomerate Member (Queen Bee). Gilligan and Suppel (1978) mapped Queen Bee at the contact between the Chesney Formation and Great Cobar Slate. That is, most cobar orebodies were deposited in the sedimentary rocks of the Cobar Super-Group.

Since the Elura area has no outcrop available for geological study, Adams and Schmidt, (1980) described the geology of the area from drill-hole data and shallow back-hoe pits. Rocks of the area are a folded, monotonous sequence of graded siltstone and shale belonging to the lower Devonian C.S.A. Siltstone unit of the Cobar Super-Group (Figure 2.2). The C.S.A. Siltstone mainly consists of quartz and muscovite with chlorite, albite, carbonate and accessory minerals pyrite, rutile and kerogen-graphite. In the area, weathering occurred and produced a porous quartz muscovite rock about 75-105 metres from the ground surface. Weathering products at or near the ground surface are mainly magnetic minerals - maghemite and magnetite.

The Elura area contains an orebody of Zn-Pb-Ag which is hosted in this rock unit. The orebody occurs with an abrupt contact to the host rock. There is no evidence to indicate the structural relationship of the host rock and the orebody. There is also no published work on the genesis of the orebody. Detailed mineralogy of the Elura orebody has been described by Adams and Schmidt, (1980).

The Elura orebody consists of siliceous, pyritic and pyrrhotitic ores. Detailed description of the mineralization of the body was made by Adams and Schmidt (1980) in the proceedings of the Elura Symposium. The orebody contains a reserve of about 27 million tonnes from the base of oxidation at 100 m to 510 m below the surface. Average density of the mineralization is about 4.2 gm/cc compared with the host rock of about 2.65 gm/cc. Pyrrhotite is the associated magnetic mineral responsible for the magnetic response in the core of the Elura body. This pyrrhotitic ore displays a high magnetic susceptibility and a high koenigsberger ratio, both of which influence the magnetization of the

zone. The natural remanent magnetization was determined to be parallel to the earth's field (Gidley and Stuart, 1980). The magnetic properties of the country rock and the mineralization of the area have been summarized in Table 2.1.

In Figure 2.3 is presented a schematic longitudinal section through the Elura orebody (After Emerson, 1980)

TABLE 2.1: *Magnetic susceptibility and koenigsberger ratio of the Elura rocks and mineralization (after Emerson, 1980)*

Rock and ore	Lithology	Magnetic susceptibility (S.I.unit)	Koenigsberger ratio ($\frac{Q}{n}$)
Weathered rock (near surface)	Quartz kaolin sericite	2.51E-04	0.1
Fresh rock (at depth)	Quartz muscovite siltstone	3.77E-04	0.1
Siliceous ore	Semi-massive to disseminated	1.25E-04	0.1
Pyritic ore	Massive pyrite	8.80E-04	0.1
Pyrrhotitic ore	Massive pyrrhotite	376.99E-04	5±

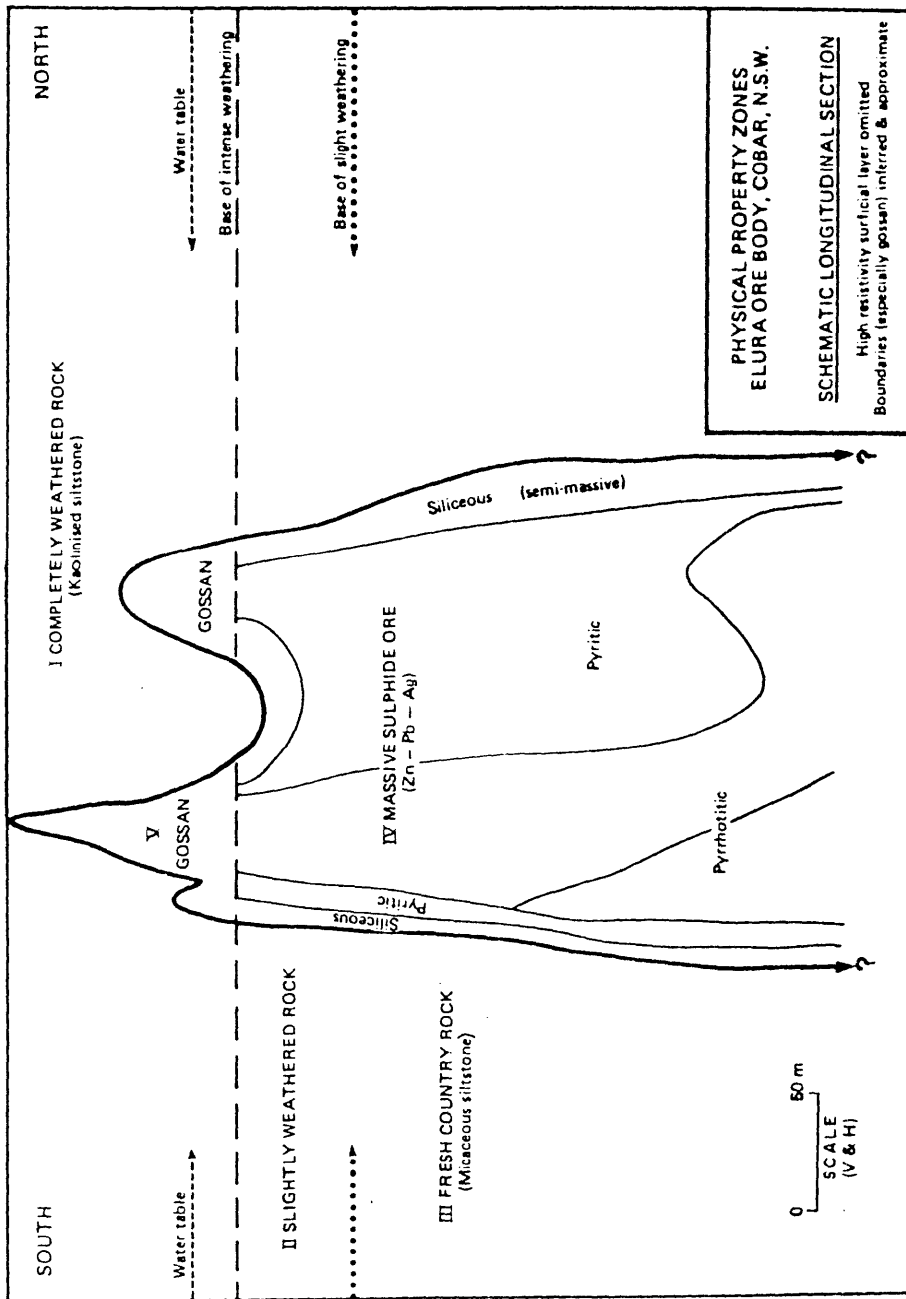


FIGURE 2.3: Schematic longitudinal section through the Elura orebody showing physical property zones (after Emerson, 1980).

2.2.2 The Near Surface Magnetic Minerals

Other magnetic minerals of significance in the area are the alluvial iron oxides occurring near the ground surface. These oxides are the principle source of magnetic noise which is the subject of this study. The magnetic susceptibility of massive grains of maghemite was measured at $346.58E-04$ (S.I. unit) and the koenigsberger ratio of 4.0 (Gidley and Stuart, 1980) was also very high.

Figure 2.4 pictures a sample of typical maghemitic gravels, collected from the ground surface. The loose rock fragments are red in colour, being stained with iron oxide. The small-sized grains in the figure are mainly maghemite, which were believed by Wilkes (1979) and Gidley and Stuart (1980) to be the main source of the geological magnetic noise. Bacon (1982) believed that the source of the geological magnetic noise above the Elura area is due to magnetite, not maghemite. Clark (1980) suggested hematite was the source of the magnetic noise. Hematite is a mineral with a very low magnetic susceptibility. However, according to Clark, hematite is found near the surface in concentrations over 30% by volume in the Cobar area. He believed it may carry a considerable remanent intensity either as CRM or TRM, giving rise to large magnetic anomalies, even though its susceptibility is very low. Hematite has a chemical composition as $\alpha - \text{Fe}_2\text{O}_3$. By chemical reaction, hematite can be reduced to form magnetite and in a reoxidation stage, magnetite will form maghemite which gives rise to a high magnetic susceptibility in soils (Le Borgre, 1960; Tite and Linington, 1975).

Maghemite (Deer, Howie and Zussman, 1964) is one form of a magnetite series. It has a chemical composition of exactly $\gamma - \text{Fe}_2\text{O}_3$, chemically similar to rhombohedral hematite ($\alpha - \text{Fe}_2\text{O}_3$). The magnetic properties of maghemite are nearly the same as magnetite. Its crystal structure, cubic spinel, cation deficient (one ninth of the iron sites are vacant) are the same as magnetite. This cubic maghemite has a high spontaneous magnetization, and a high magnetic susceptibility. Maghemite cannot be distinguished from magnetite by x-ray diffraction. Pure maghemite may be chemically distinguished from magnetite by the absence of Fe^{+2} , if it can first be separated (magnetically or



FIGURE 2.4: *Examples of loose rocks (left hand side), maghemite, and magnetite minerals (small grains) collected from Cobar ground surface.*

otherwise) from other iron oxides.

Maghemite collected from the Cobar area is well-rounded and brown or dark brown in colour (Figure 2.4). In transmitted light, under a microscope (Deer et al., 1964) maghemite is brown to yellow, and by reflected light it appears white or grey-blue with a high reflectivity.

According to Deer et al. (1964), natural maghemite usually derives from the supergene alteration of magnetite deposits. Maghemite may be formed from other iron oxides by the reducing action of organic matter or by the dehydration of lepidocrocite. $\text{Fe}(\text{OH})_2$ may oxidize to the ferric species near the surface by the addition of O_2 to yield lepidocrocite which then dehydrates to maghemite.

Bacon and Elliot (1981) explained the formation of maghemite by redox chemical remanent magnetization and proposed that the reduction taking place near the upper end of the sulfides can produce magnetite, which by later lower temperature oxidation goes to maghemite.

Alternatively, it was proposed by Baker (1978) and Davis (1980) that maghemite may be formed by the intense leaching of the pre existing rocks, accompanied by the accumulation of iron oxide in favourable chemical and physical locations or as the erosional product of lateritic iron deposits.

Maghemite, according to Stacey and Banarjee (1974), is normally stabilised by impurities, resulting in much higher transition temperatures up to and above 600°C . Pure maghemite is unstable at temperatures above 300°C (Grant and West, 1965), at which temperature it converts spontaneously to hematite ($\alpha\text{Fe}_2\text{O}_3$) which has a rhombohedral structure and is a fundamentally antiferromagnetic mineral.

While there remains some controversy as to the actual analysis of the minerals responsible for the near surface magnetic noise, it is not in doubt that the noise source is the iron-rich alluvial pebbles observed near the ground surface throughout the Cobar region. This

study is concerned with the magnetic characteristics of these deposits rather than their mineralogy.

2.2.3 Maghemitic Palaeochannels

The maghemitic palaeochannels deserve a special mention because they present a particularly difficult problem to exploration in the region. While the magnetite, maghemite and hematite minerals are widely distributed as aeolean and alluvial deposits, they also occur in an extensive network of well developed palaeochannels. There still remains some controversy as to whether the maghemitic gravels have been gravimetrically sorted into these channels by hydraulic processes or whether they in fact form in the wet chemical environment of the channel.

Whatever the origin of the maghemitic palaeochannel, the properties remain the same. Along the extent of the channel, a very high concentration of maghemite occurs. In many cases the channels are several hundreds of metres wide, extend for many kilometres and contain deposits of maghemite minerals up to several metres thick. The physical dimensions of these intense magnetic sources present the worst case of noise characteristics where the target signal was expected to ~~originate~~ ^{originate} at approximately 100 metres depth.

Many of the airborne magnetic survey anomaly targets were found to occur over maghemitic channels. Quite frequently, only the ~~thickest~~ ^{thinnest} deposits along the channel were observed as aeromagnetic anomalies and so their association with a palaeochannel was not recognised until ground exploration was conducted. Where aeromagnetic anomalies were found to coincide with a palaeochannel exploration usually ceased. The assumption that the channel deposit was the source of the anomaly may not always have been valid, but in the absence of an economically viable means of exploring beneath the channel the assumption above was usually adopted. It is because much of the palaeochannel area has remained effectively unexplored that this particular exploration problem has been considered as the final test of merit for the exploration procedure developed in this study.

2.3 Conclusion

From the study of the Elura environment, it is shown that magnetic exploration methods can be applied to the Elura area but widespread occurrences of magnetic materials at or near the surface will cause difficulty in recognizing magnetic anomalies which may be masked by those of magnetic noises. The use of magnetic method in this area requires a technique which must be able to be used to obtain magnetic signal with least magnetic noises for magnetic interpretation. To obtain magnetic signal with less noise, the technique must involve with data collection and data processing which will be explained in Chapter 4, 5 and 6.

Before going to understand the separating technique of magnetic signal and noise, definition of signal and noise characteristics will be described in the next chapter to know what magnetic signal and noise are.

Chapter 3

DEFINITION OF SIGNAL AND NOISE CHARACTERISTICS

3.1 Introduction

The old phrase 'one mans signal is another mans noise' is particularly relevant to the study and this chapter defines the 'signal' and 'noise' as appropriate to the present situation of deep magnetic targets obscured by intense near surface magnetic interference. In particular it is necessary to emphasize that many of the magnetic variations defined here as noise have the characteristics of high amplitude and significant width which would be considered as 'signal' in a different geological environment. Similarly, the description of a magnetic 'spike' in this context refers to an intense magnetic anomaly of narrow (but finite) width.

3.2 Definition of Signal Characteristics

3.2.1 General description

Implied in this study is the assumption that the source of magnetic 'signal' will be either major, deep geological structural features such as lithological boundaries or major faults, or base metal mineralization of economic dimensions which contain sufficient pyrrhotite as to make them a magnetic target. In the Cobar environment, economic mineralization previously discovered has always contained a magnetic mineral component (Davis, 1980). In chapter 7, the magnetic

signal arising from a theoretical mineral target occurring at a range of depths below surface has been calculated in an attempt to generalize the potential depth to which an economic magnetic target might be detectable in the Cobar environment.

The present study has concentrated upon the Elura orebody as a guiding case study. The magnetic signal from this orebody can be quantitatively defined.

3.2.2 The Elura magnetic signal

With the drill control available, it was possible to quite accurately model the magnetic signal arising from the Elura orebody. The spectrum of this signal was quantifiable. The measured signal, presented in chapter 6 was compared with that expected from theoretical modelling.

A longitudinal cross section through the Elura orebody was presented in Figure 2.2. The pyrrhotite zone was considered to be principally responsible for the magnetic anomaly of the body. The pyrrhotite zone was represented by the simplified two-prism model given in Figure 3-1(b).

This anomaly curve was computed by using a computer program written by Clark (1981) in FORTRAN IV for the University of New England's DECSYSTEM-20 computer. The program used in the calculation is based on a formulae given by Bhattacharyya (1980) and assumes that component bodies are right rectangular with a uniform magnetic susceptibility contrast.

The calculated magnetic anomaly across the centre of this model (line 50850N of the survey grid) was also given in Figure 3.1(a).

The spectrum of the computed anomaly curve was calculated using a Fast Fourier Transform (Appendix II) Figure 3.2. Note that the spectrum is totally contained within the frequency range of 0 to 0.0055 cycles/metre and that close to 95% of the spectrum lies within the frequency range of 0 to 0.003 cycles/metre. (See Chapter 6.7).

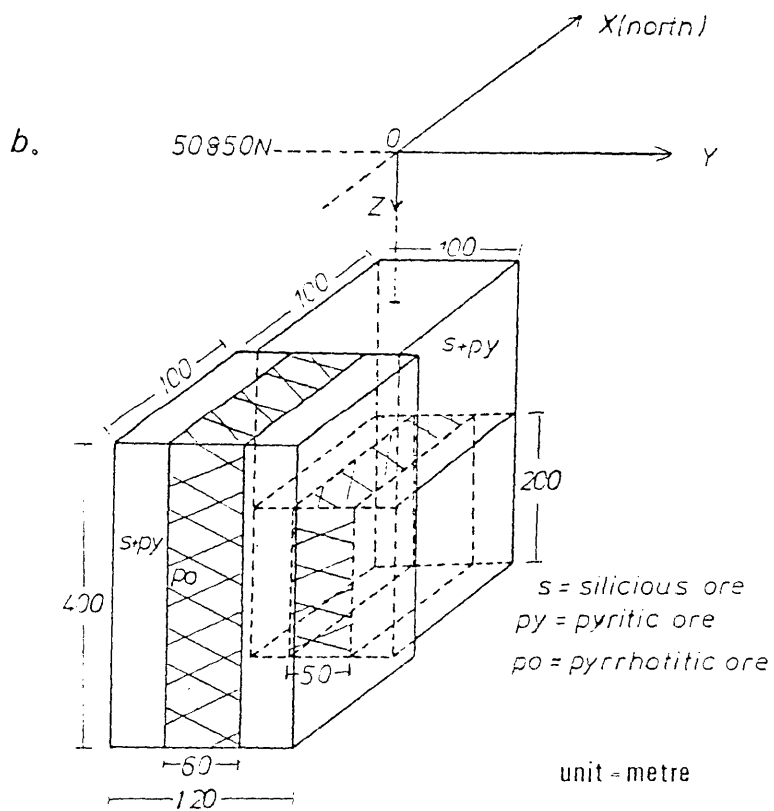
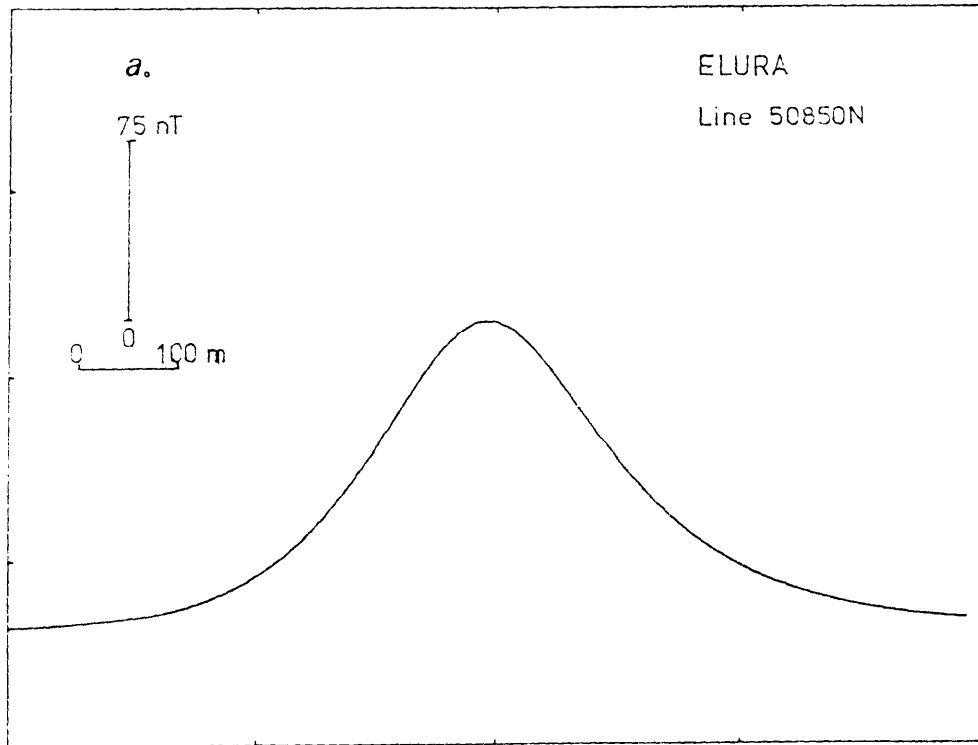


FIGURE 3.1: Plot of the Computed anomaly curve (a) arising from the model (b) representing the pyrrhotite zone of the Elura orebody.

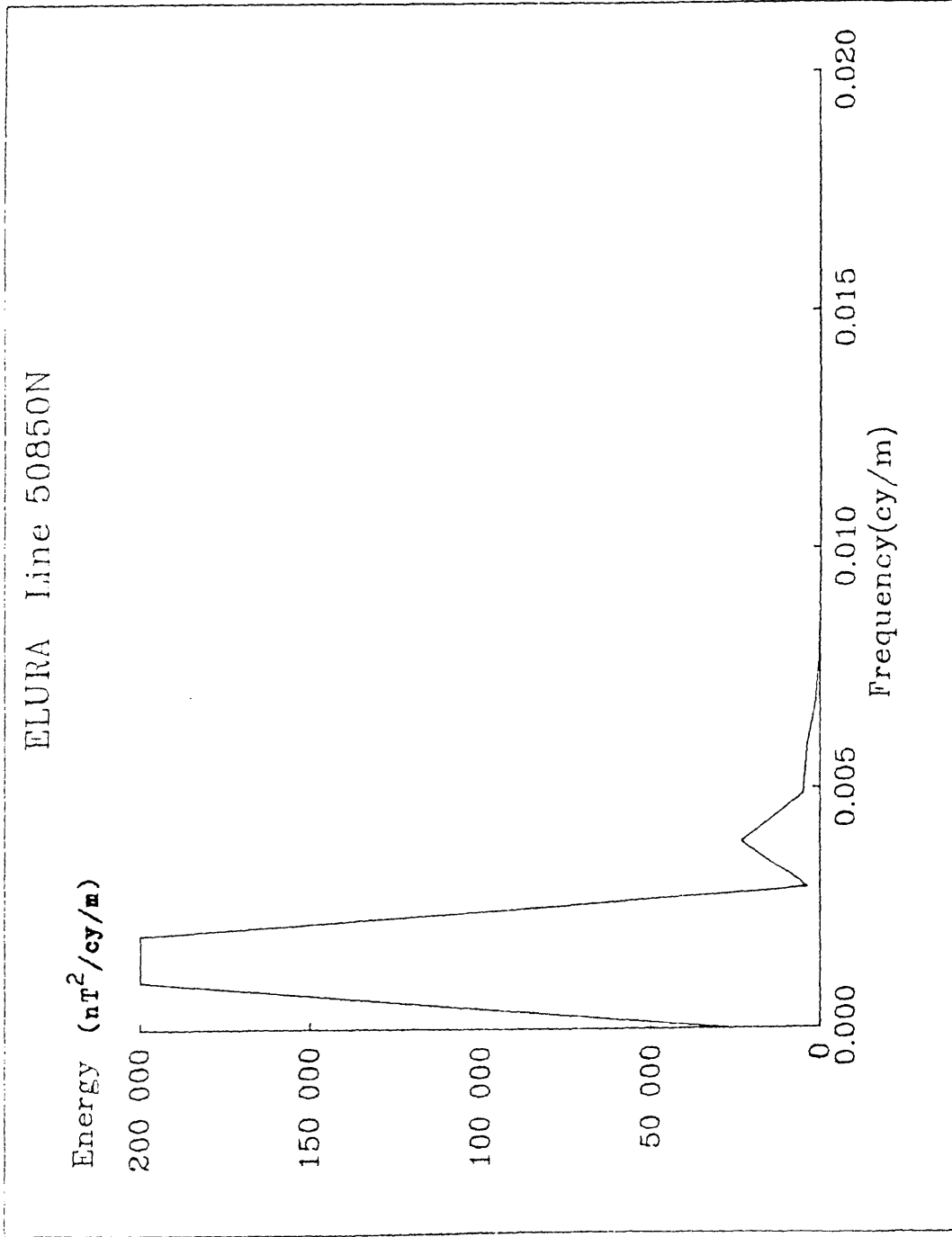


FIGURE 3.2: Plot of the signal energy spectrum of the computed anomaly curve arising from a model representing the pyrrhotitic zone of the Elura orebody. The anomaly curve was calculated corresponding to grid line 50850N across the centre of the orebody.

The energy spectrum was also calculated for the Elura mineralization model assuming a range of depths beneath ground surface. A plot of these spectra is given in Figure 3.3. Note that the effect of depth on the spectrum is to attenuate the amplitude with greatest attenuation effecting the highest frequencies. At a depth of 600 metres the signal is almost entirely confined to the 0 to 0.002 cycles/metre range while at a depth of 50 metres the spectrum is still predominantly in the 0 to 0.005 cycles/metre range.

The behavior of the signal spectrum with depth is important when consideration is made of the maximum depth to which the body may be expected to be detected by magnetics. It is also important when considering the relative merits of conducting airborne magnetic exploration or ground level in relation to the two exploration philosophies presented in Chapter 1.

3.3 Sources of Near Surface Magnetic Noise

3.3.1 Cultural noise sources

Mining areas are frequently characterized by the scatters of pioneers ~~debris~~ ^{debris} including steel drill rods, remnants of old machinery, discarded habitation artifacts and an abundance of steel food cans. Farm remains include steel fence posts, scraps of wire and miscellaneous machinery. As geophysical techniques develop there is often good reason to reexplore areas adjacent to known mining sites. In some cases exploration is required through presently occupied habitation areas where steel objects are common. This study deals with near surface, intense noise sources such as those produced by cultural steel objects. While the anomaly due to a motor vehicle has a finite width of several metres, in the context of this study, the anomaly constitutes a noise 'spike'. Extreme amplitude, finite width spikes of this form are the subject of special attenuation in this study.

Because of the extreme amplitude of such spikes, their spectrum contains significant energy over a very wide frequency range including that occupied by the 'signal'. Such extreme amplitude features

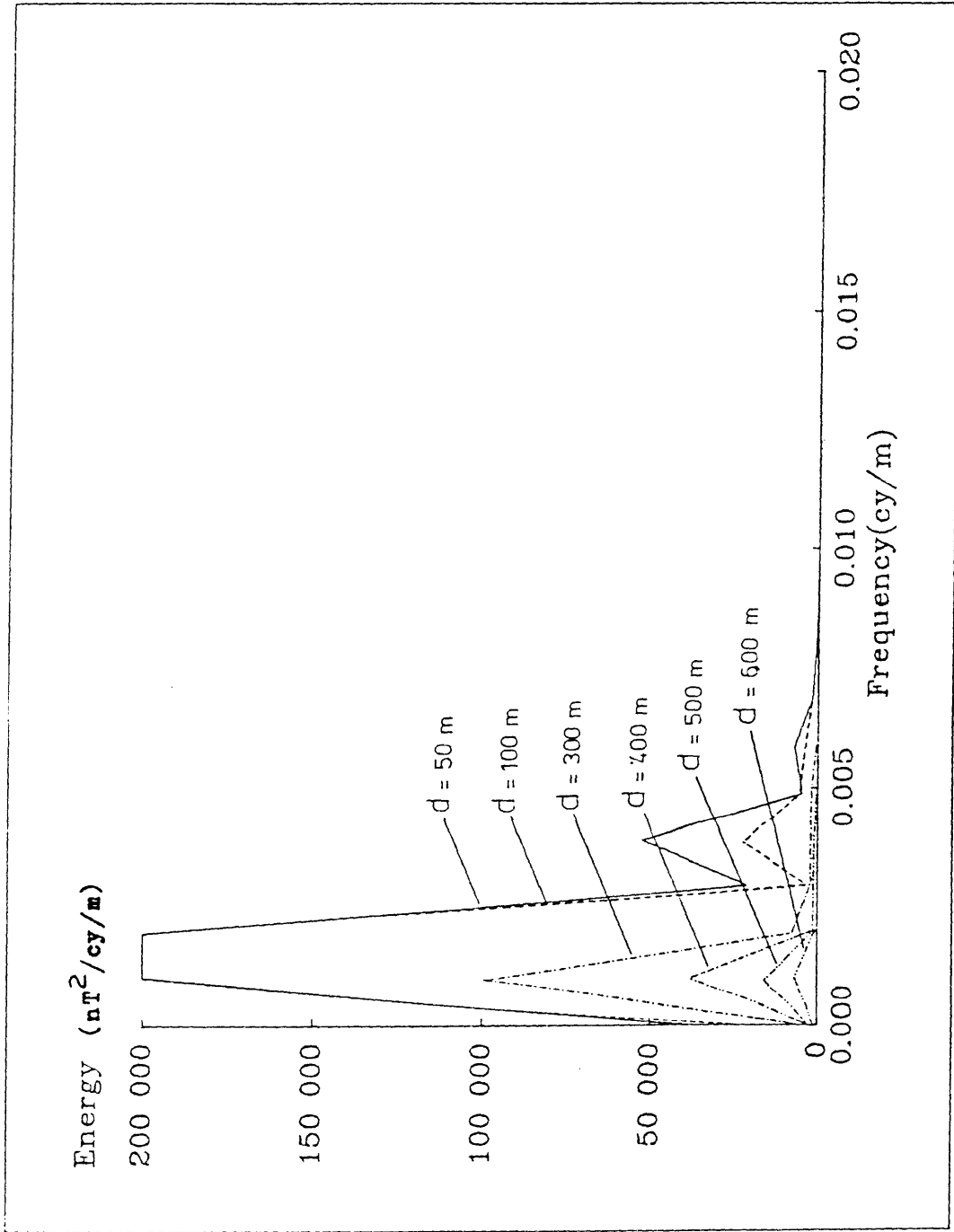


FIGURE 3.3: Signal energy spectra of the Elura model placed at a range of depths beneath ground surface.

however can be readily recognised by their high amplitude and narrow width, and, having been identified, may be deleted from the data. This procedure was discussed in Chapter 5.

3.3.2 Basalt Flow

A common source of near surface intense magnetic interference is the thin basalt flow. Many basalts contain highly inhomogeneous concentrations of magnetite. Jointing, flow boundaries and weathering provide randomly oriented zones of intense induced and remanant magnetization. The magnetic profile over a basalt flow will therefore display a broad band spectrum with the low frequency component originating primarily from local very high amplitude features considered here as spikes.

3.3.3 Maghemitic Gravels

The composition and occurrence of maghemitic gravels has been discussed. The intense magnetization and small physical dimensions of each gravel grain give rise to a high frequency spectral component. Local concentrations of gravels give rise to extreme amplitude narrow width anomalies which contain significant energy in the low frequency end of the spectrum.

3.3.4 Similarities between different noise source spectra

The three near surface noise sources discussed above all display the same characteristics. The localized nature of the individual magnetic components gives rise to a wide spectral range in the high frequency end. Larger, cultural steel objects, zones of magnetite differentiation in basalts and local concentrations of maghemitic gravels each give rise to peak magnetic anomalies of several thousand nT amplitude over areas of up to 10's of metres. The spectrum of these 'spikes' is very broad band and contains significant energy in the low frequency 'signal' end of the spectrum.

In this study area there is an absence of basalt flow, but in places there was cultural interference from drilling and other exploration activities. The two noise sources were indistinguishable in

their characteristics. The analysis of signal and noise presented here considered only the maghemite noise but the significance of the study to exploration beneath thin basalt and in areas of human habitation was not overlooked. The very similar spectral characteristics of the three noise sources make the results of this study applicable to all three situations.

3.4 Definition of Noise Characteristics

3.4.1 General description of noise from maghemitic gravels

A magnetic profile was selected from an area which was known to be barren of deep mineral or geological signal source. The line was 50450N on the Elura survey grid. Figure 2.5 shows the magnetic profile sampled at 0.25 metre intervals.

The character of the spectrum of the magnetic profile from line 50450N was displayed in Figure 3.5. The low frequency segment of this spectrum was expanded in Figure 3.6 as this frequency range includes that in which the target signal spectrum would also be expected to fall.

3.4.2 Extreme amplitude, short wavelength noise components

Examination of Figure 3.4 reveals several very high amplitude, short wavelength features. These arise from very localized high concentration of maghemitic pebbles. However, they closely resemble the magnetic anomaly arising from a cultural steel object or magnetite enriched joint in basalt. These spike-like features can be several thousand nT in amplitude and may extend over a width of 10 or 20 metres. Their importance lies in the fact that their spectrum is very broad band and contains significant energy in the signal band. They can however be positively recognized from the magnetic profile even though their low frequency spectral component is indistinguishable from signal. For this reason it was necessary to devise an automatic or semi automatic procedure for identifying these spike-like components of the noise, and replacing them, BEFORE spectral processing of the data can be performed.

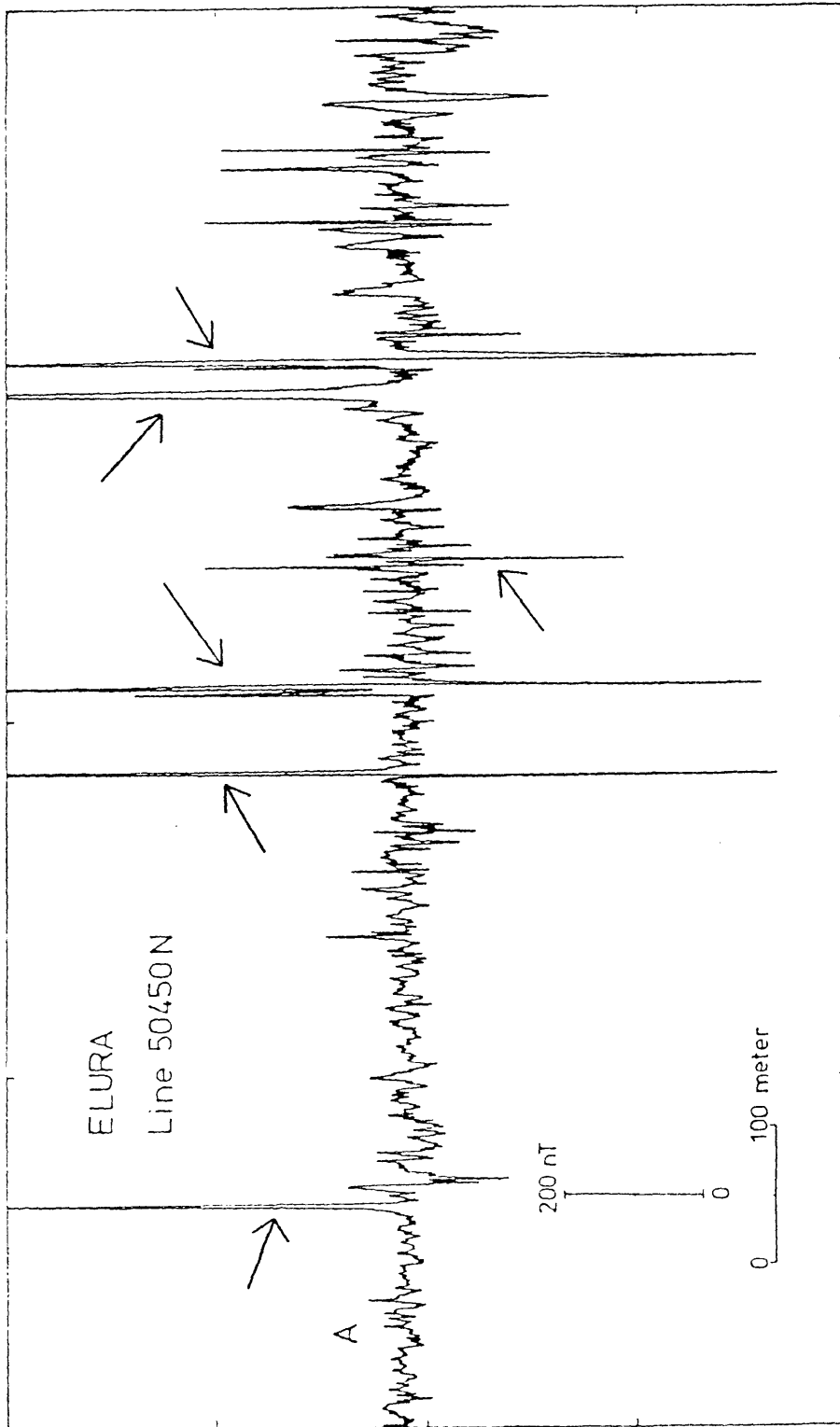


FIGURE 3.4: Magnetic profile recorded in an area known to be barren of deep mineralization or geological signal sources. The area did have a typical thin cover of maghemitic gravels. Extreme magnetic noise features (arrowed) arise from local concentrations of maghemitic pebbles (they also closely resemble interference from cultural steel objects near the ground surface).

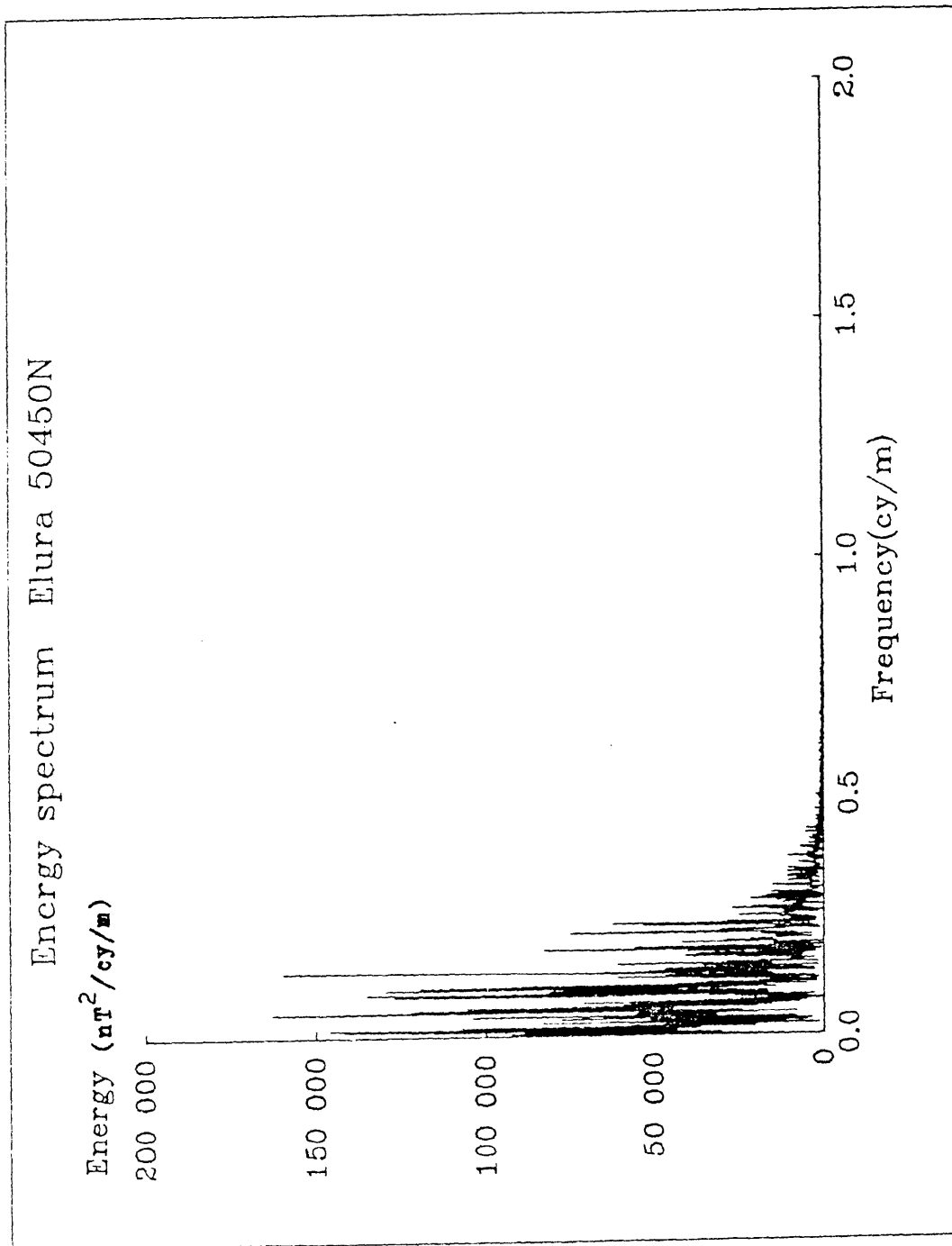


FIGURE 3.5: Noise energy spectrum of a typical magnetic profile recorded in an area barren of deep mineralization but covered with a thin spread of magnetic gravels.

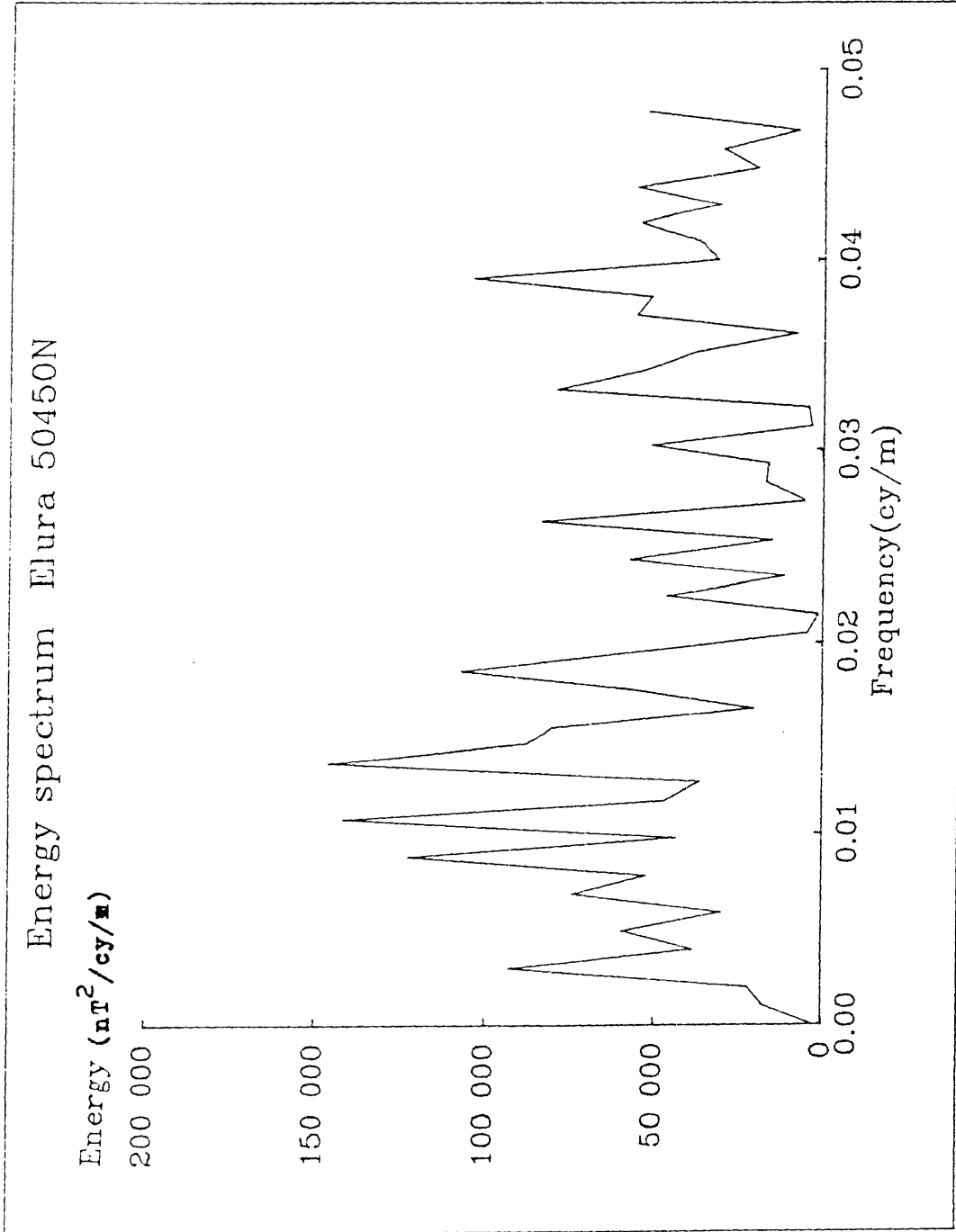


FIGURE 3.6: Plot of the low frequency noise energy spectrum of a magnetic profile recorded in an area barren of deep mineralization but covered with a thin spread of maghemitic gravel.

3.5 Conclusion

Signal and noise characteristics of the Elura area can be defined. The spectrum of the Elura magnetic signal is confined at the low frequency end within the frequency range not more than 0.0055 cycles/metre for the depth of the magnetic model body of 100 metres. Noise spectrum shows several very high amplitude and short wavelength features in the frequency ranges includes the significant energy of the signal band. These signal and noise can be separated if an auto-tic or semi automatic procedure is used. Before going to this procedure, technique of magnetic separation will be considered and started from data collection which will be explained in the next chapter.

Chapter 4

MAGNETIC SURVEY DESIGN IN REGIONS OF INTENSE NEAR SURFACE NOISE

4.1 Introduction

The parameter most influencing the design of a magnetometer survey are the spectra of the signal and noise and the relative amplitude of each. Not only was the survey grid required to adequately sample the target (the conventional philosophy on this subject) but because of the large relative amplitude of the noise waveform, the survey was required to adequately sample this also. Thus the spectrum of the total magnetic waveform needed to be examined before the appropriate sampling parameters could be defined. This applied equally to the design of airborne surveys as to ground level ones. Sampling interval requirements, signal and noise amplitudes and the amplitude of magnetic gradients were important considerations in the specification of magnetometer instrumentation.

4.2 Sampling Parameters

4.2.1 Sensor elevation

As outlined in the statement of objectives, a philosophical thrust of this study was the quantitative assessment of ground level versus airborne surveying as strategies for magnetic exploration beneath a near surface noise source. In Figure 4.1 is presented the spectra of a magnetic noise profile (Elura line 50450N) computed for a

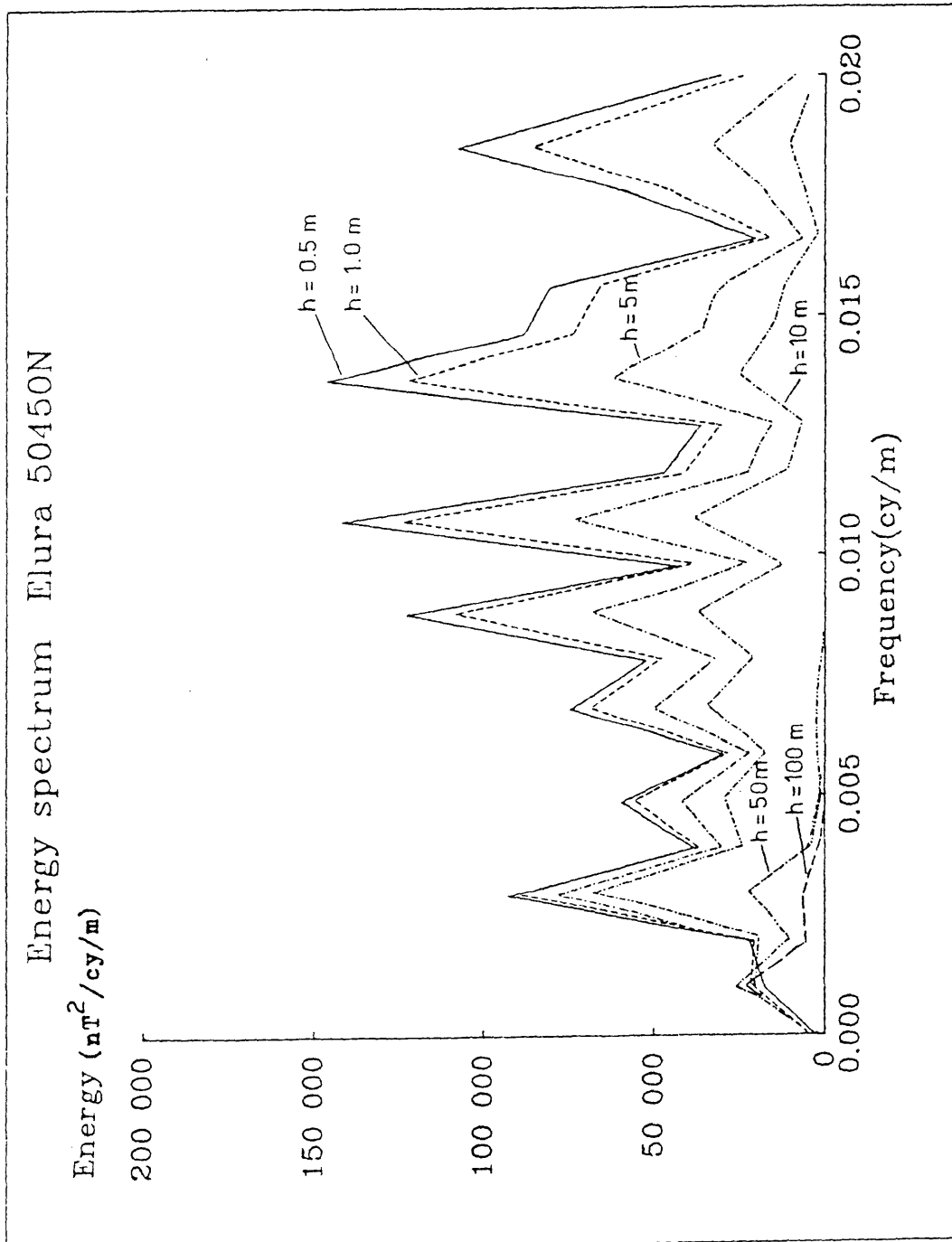


FIGURE 4.1: Noise energy spectra of Elura line 50450N computed for different sensor heights above ground.

range of sensor elevations above the noise source. Most apparent from this data was the fact that increasing the sensor height above the noise source dramatically attenuated the high frequency component of the spectrum while having little effect on that part of the spectrum in which the signal would lie. This observation was important for two reasons. Clearly the higher the sensor elevation the wider can be the sample spacing while still adequately sampling the waveform. Also noticed was the fact that increased sensor elevation did not significantly attenuate the noise energy in the signal waveband. Thus any attenuation of a signal amplitude at a greater rate than that occurring to the low frequency component of the noise would result in a deterioration of the signal to noise ratio. This possibility was examined in detail in Chapter 6.

4.2.2 Data Sample Interval

At least two samples per shortest component wavelength are required to define all frequency components of the waveform. (Blackman and Tukey, 1958). This is known as the 'sampling theorem'

Sampling is very important in data processing. If the data sample interval is not close enough, aliasing problems will be met. Several methods are available to minimize aliasing. The simplest is to choose the sample interval sufficiently small so that processed signals will have very little energy above the associated folding frequency or Nyquist frequency. The Nyquist frequency is the frequency which is equal to half the sampling frequency. Frequencies greater than the Nyquist frequency will alias as lower frequencies from which they will be indistinguishable. Aliasing can be simply pictured by the following example.

Let Δx be a unit length sample interval, then the Nyquist frequency is $1/2\Delta x$ cycle per unit length. A continuous signal in Figure 4.2a is in a band-limited spectrum $F(S)$. The spectrum is zero outside the frequency range $-S_C, S_C$. For simplicity of graphical representation, let the spectrum $F(S)$ be real, so the evenness of $f(x)$ has been introduced. Now, digitize the function $f(x)$ with a sample interval

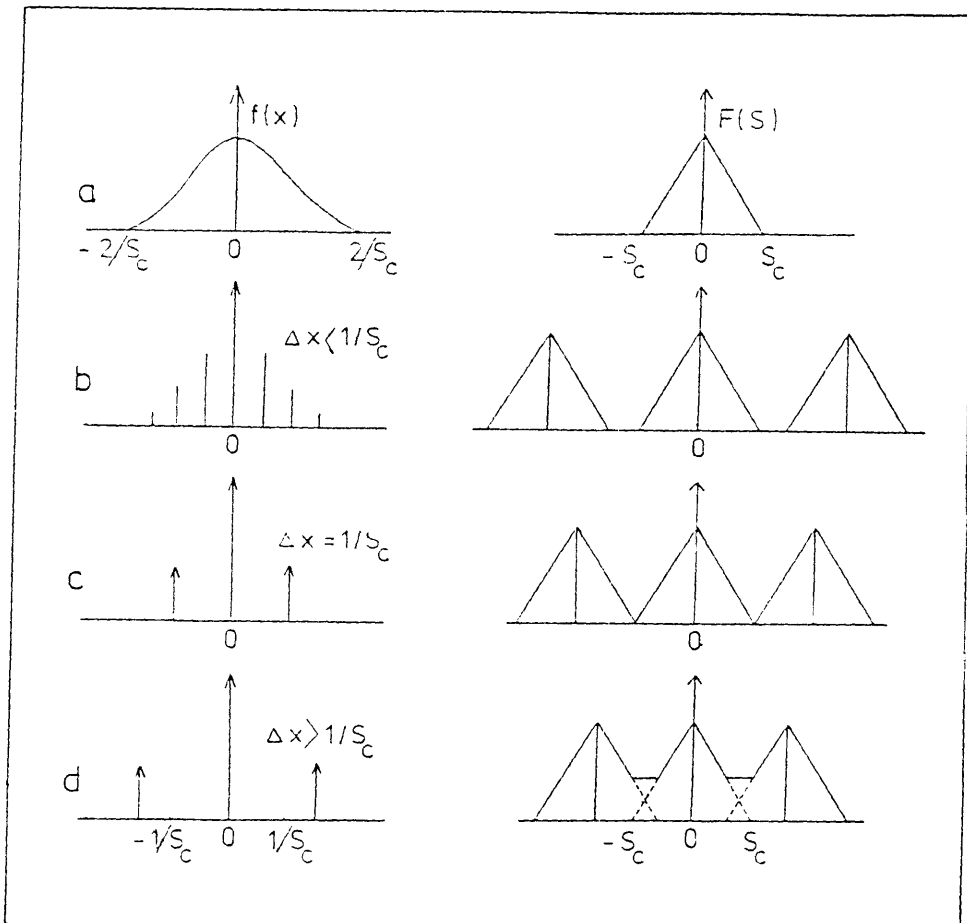


FIGURE 4.2: Influence of the sampling length of the spectrum of the output (after Ota Kulhanek, 1976).

Δx less than $1/S_c$, see Figure 4.2c. Then, apart from the normalizing factor $1/\Delta x$, repetitive components are separate, perfect copies of the input spectrum. That is, full recovery of the input has been achieved. If the sample interval is increased up to the limit length, $\Delta x = 1/S_c$, Figure 4.2c will show a similar picture. But if the sample interval is larger than $1/S_c$, overlapping of the spectrum will occur, see Figure 4.2d. The recovery of the input signal from the distorted output spectrum is then no longer possible. That is, a function whose spectrum is band-limited is fully specified by samples spaced at equal intervals not more than $1/S_c$. In other words, the highest frequency which can be reproduced from data sample with the sampling length Δx is $1/2\Delta x$.

4.2.3 Relationship between sensor height and sample interval

From figure 4.1 it can be seen that for a sensor elevation of 100 metres the sample interval should be 2×0.005 measurements per meter (or 100 metres). For an elevation of 50 metres the sample interval must be no greater than about 60 metres. From Figure 3.5 when the sensor elevation was 0.5 metres a sample interval at about 1 metres is required.

As a rule of thumb:

"The Sample Interval Should Not Exceed Approximately the Elevation of the Sensor Above A noise Source".

Examination of sample intervals and aliased energy in more detail provided the following.

Let us use mathematics very similar to that described by Bhattacharyya (1966) to express the energy spectrum, $E(v)$, of the magnetic profile due to a prism in one variable from (Green, 1972). A rectangular coordinate system is assumed, see Figure 4.3, where the X -axis is taken to be coincident with the profile line and at an angle θ with respect to geographic north (θ is positive when measured clockwise from north) and the prism extends to \pm infinity in the Y -axis direction. Now, the expression is:

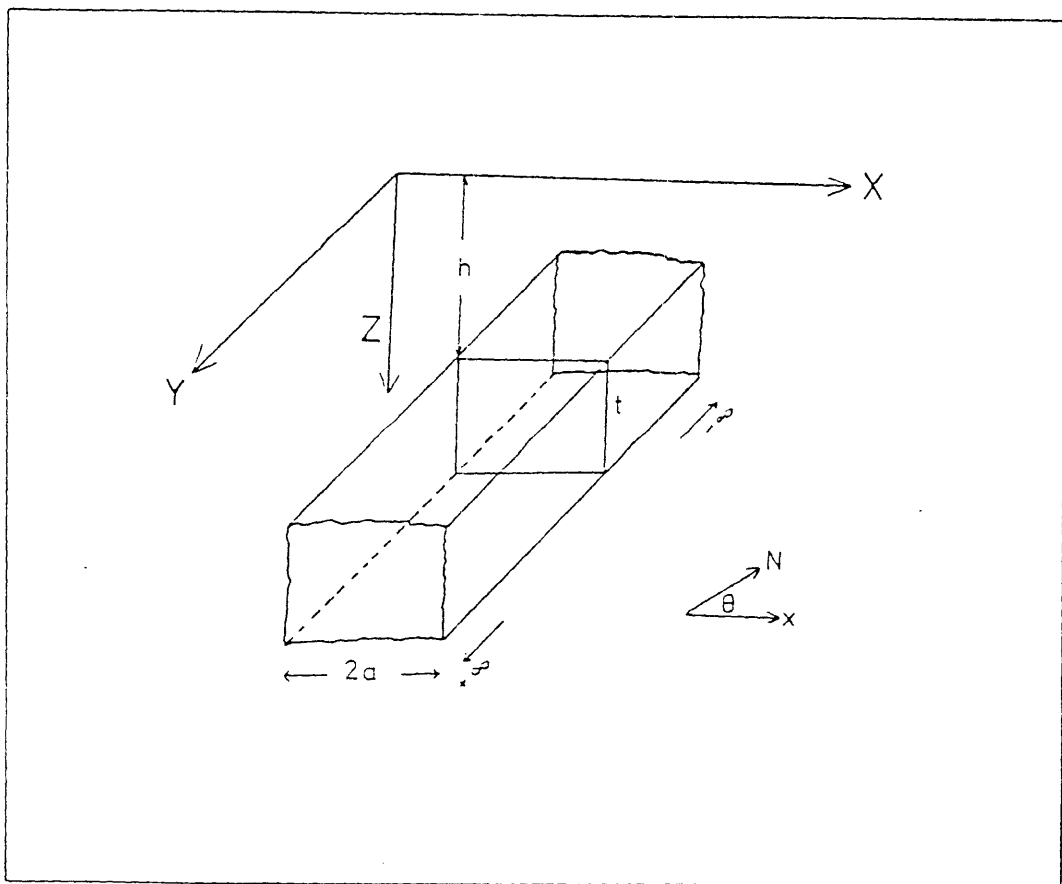


FIGURE 4.3: Diagram of two-dimensional body used as the base model for the expression of the energy spectrum (taken from Green, 1972).

$$E(v) = 4\pi^2.K^2.R_1.R_2.W.T.H \quad (4.1)$$

where $K/2a$ = the magnetic moment/unit volume,

$$R_1 = \sin^2 I_1 + \cos^2 (D_1 - \theta) . \cos^2 I_1 ;$$

I_1 = the inclination of the geomagnetic field vector,

D_1 = the declination of the geomagnetic field vector,

$$R_2 = \sin^2 I_2 + \cos^2 (D_2 - \theta) . \cos^2 I_2 ;$$

I_2 = the inclination of the magnetic moment vector,

D_2 = the declination of the magnetic moment vector,

$$W = \left(\frac{\sin(va)}{va} \right)^2 ; \quad (4.2)$$

W = a geometrical factor of the body,

v = the angular wavenumber equivalent of the space variable x and $2a$ is the width of the prism,

$$T = (1 - \exp(-tv))^2 ; \quad (4.3)$$

t = the thickness of the body,

$$H = \exp(-2hv) ; \quad (4.4)$$

h = the depth to the top of the body

If we consider the energy spectrum in terms of depth to the top of body only and leave other parameters constant, then, the expression can be rewritten as:

$$E(v) = C.H$$

where $C = 4\pi^2.K^2.R_1.R_2.W.T.$

or

$$E(v) = C \exp(-2hv) \quad (4.5)$$

According to the sampling theorem (Bracewell, 1978), the shortest spatial wavelength or Nyquist wavelength, L_n is equal to twice the sample interval, that is,

$$L_n = 2\Delta x$$

where Δx is the sample interval. Then the Nyquist frequency is:

$$f_n = \frac{1}{L_n} = \frac{1}{2\Delta x} .$$

Any wavelength shorter than L_n is aliased into a wavelength longer than L_n (Blackman and Tukey 1958). The aliased energy spectrum can be estimated from the relationship of the sample interval and the sensor height. The relationship is obtained by calculating the fraction of the aliased energy spectrum. From equation (4.5) we have:

$$E(v) = C \cdot \exp(-2hv) .$$

The aliased energy spectrum, $E_a(v)$ is the fraction of the energy spectrum from the Nyquist frequency to infinity. The aliased energy spectrum can be written in mathematical form as:

$$E_a(v) = \left[\int_{v_n}^{\infty} E(v) dv \right] \div \left[\int_0^{\infty} E(v) dv \right] \quad (4.6)$$

where $v_n = 2\pi f_n$,

$$= 2\pi \frac{1}{2\Delta x} = \frac{\pi}{\Delta x} .$$

If the numerator of equation (4.6) equals zero, then aliased energy spectrum is zero. Evaluating equation (4.6), we have:

$$E_a(v) = \exp\left(-\frac{2\pi h}{\Delta x}\right) . \quad (4.7)$$

The fraction of the aliased energy spectrum, $E_a(v)$ is therefore dependent upon the sample interval and the sensor height. If the sensor height is constant, the percentage of the aliased energy spectrum increases with the sample interval, see Figure 4.4 and Table 4.1. Theoretically, for a 5% maximum value of the aliased energy spectrum, then the sample interval must not exceed one metre for the sensor height of 0.5 metre, or two metres for a sensor height of one metre, or four metres for a sensor height at two metres. Not all of the aliased energy will necessarily occur in the signal bandwidth and hence the figure of 5% represents the maximum value. For a 1% maximum value of aliased energy the previously stated rule of thumb is appropriate (P. 35).

TABLE 4.1: *Fraction of aliased energy spectrum at different sample intervals and sensor heights*

Δx (metres)	$E_a(v) \%$		
	$h = 0.5 \text{ m}$	$h = 1.0 \text{ m}$	$h = 2.0 \text{ m}$
0.25	3.49E-04	1.22E-09	1.48E-20
0.50	0.19	3.49E-04	1.22E-09
1.00	4.32	0.87	3.49E-04
2.00	20.79	4.32	0.19
3.00	35.09	12.32	1.52
4.00	45.59	20.79	4.32
5.00	53.35	28.46	8.10
10.00	73.04	53.35	28.46

4.3 Instrumentation Requirements

4.3.1 Airborne Systems

Airborne magnetic systems are now routine and a description of necessary navigation control and data logging facilities is not appropriate. However some relevant statements can be made. Except for

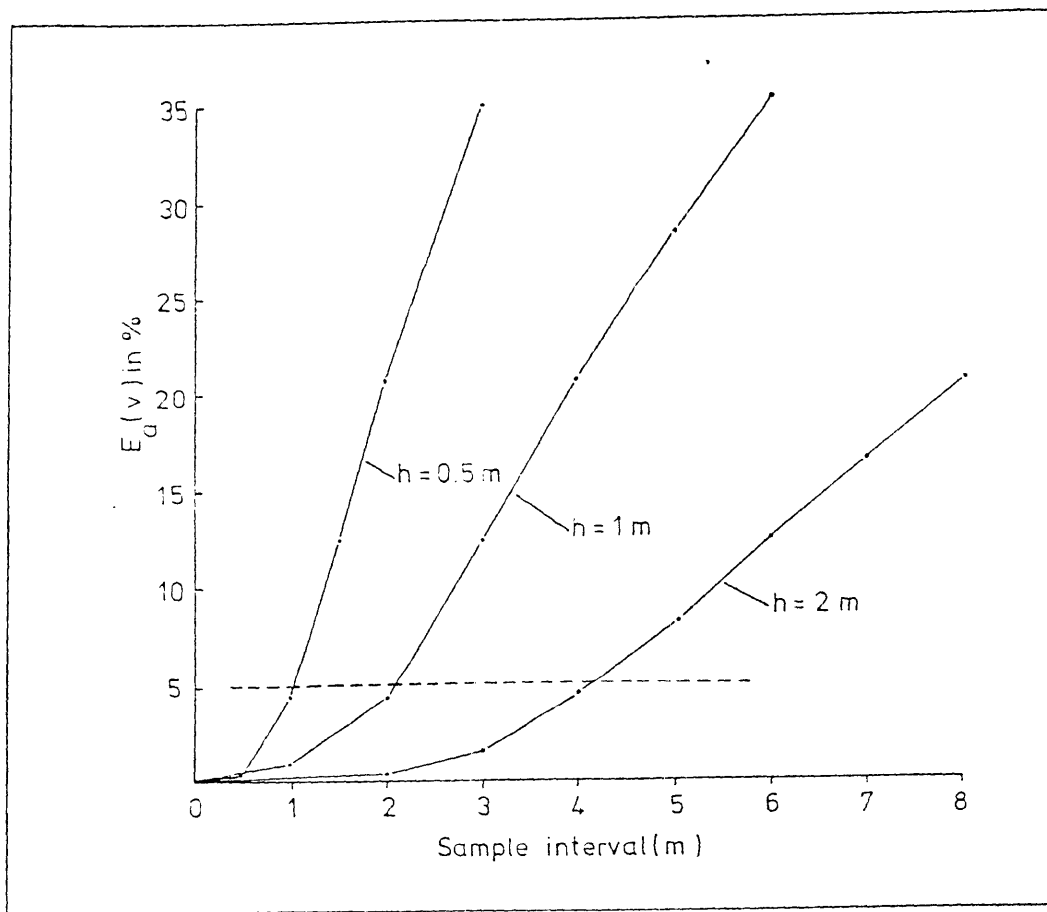


FIGURE 4.4: Graph of fraction of aliased energy spectrum against data sample interval with the sensor heights at 0.5, 1 and 2 metres.

very low level surveys (say 20 metres elevation) as may be conducted by helicopter systems, the magnetic gradients over intense magnetic or cultural noise sources would not be expected to seriously degrade a proton precession resonance signal. The sensitivity of the proton precession magnetometer can be described as adequate given that the noise waveform amplitude at 100 metres was still of the order of 1 nT. Given that the optimum flying elevation for an airborne survey (see chapter 6) was approximately 70 metres, we deduce that the maximum sample interval would be about 70 metres and this specification can be met without resorting to the more rapid sampling caesium magnetometer. Economics may be achieved by flying a caesium system at a faster surface speed.

4.3.2 Ground level magnetometer system

We have previously defined the necessity of sampling data at intervals of less than the sensor elevation. The logistics of performing a proton precession magnetometer survey at this sample interval are prohibitive on a routine basis because of the long polarization time (up to 3 seconds) of most proton precession magnetometers. Moreover long polarization times are demanded because of the degradation of the precession signal due to the high magnetic gradients encountered close to magnetic noise sources. In fact, in many areas including but not restricted to, the magnetic palaeochannels, the proton precession magnetometer will simply not tolerate the steep gradients.

It was not until the development of the caesium vapour magnetometer that a solution to the problem of magnetic exploration in regions of intense near surface magnetic noise became practical.

The magnetometer system used in this study was developed by Stanley (1975 a,b, 1982) It was described by Stanley (1982) as follows.

"Telemag is an instrument which enables total magnetic field or magnetic gradient measurements to be automatically recorded at uniform close distance intervals while continuously traversing the ground. The system is hand held, fully portable and enables measurements to 0.1 nT or 0.05 nT/m to be recorded at a rate of up to 11 per second. When translated to survey speed, this means that measurements taken

at 0.25 metres intervals can be recorded at up to 10 km/hr or 5 cm sample intervals at up to about 0.5 m/sec. The instrument can be use as a self-contained mobile, as a mobile which is synchronously radio-linked to a base (i.e. diurnal cancelling difference magnetometer) or as a gradiometer.

The system consists of a caesium magnetometer sensor (two sensors for a gradiometer), a digital display, an audio tone varying with the magnetic field value, a coder employing an audio frequency digital code suitable for transmitting data via CB radio or direct recording on cassette tape, an automatic distance measuring device using cotton thread and a decoder with digital and analog output part. After a preselected distance increment has been traversed the magnetic field or gradient measurement is automatically initiated, its value coded and either transmitted via radio to a base data acquisition system or directly recorded on cassette. Telemag is the only digital magnetometer system presently capable of viably recording magnetic data at the survey density required to define small (archaeological) targets. This advantage is particularly important in Australian conditions where short wavelength geological noise sources must be separated from the (archaeological) signal.

MODES OF OPERATION

1. As a self-contained mobile magnetometer with one or two man operation automatically recording profiles at continuous walking speed. The operator has immediate feedback as to the presence and location of anomalies through the audio monitor and digital display.
2. As a self-contained gradiometer - as above but with two man operation for convenience.
3. As a hand-held mobile synchronously linked by radio or cable with a base station magnetometer for micropulsation cancelling 'difference' magnetometer operations. The base station usually consists of a vehicle-borne data-processing facility.
4. As a rapid 'search' device in which the operator only relies on feedback from the audio monitor to locate specific objects, i.e. no data recording."

In areas of open terrain such as Elura the magnetometer can be operated from a moving vehicle. To protect the caesium sensor from shock and vibration and to isolate it from interference from the



FIGURE 4.5: *Vehicle-borne caesium vapour magnetometer and recorders - analog and cassette tape recorders - housed in the car.*

vehicle, it was hand carried by person walking 30 metres behind the vehicle. The sensor was connected to the vehicle borne system by coaxial cable which served both to send the magnetic signal to the vehicleborne recorder and also to maintain a constant separation between sensor and vehicle.

The vehicleborne instruments (see figure 4.5) included a digital odometer coupled to the vehicle gearbox. This odometer was calibratable to allow for tyre size and terrain conditions. Also included was a chart recorder on which the magnetic profiles were proportionally plotted at programable horizontal scales.

It should be noted that the principle advantage of the caesium magnetometer in this application was not its high resolution (0.1 nT) but its tolerance to steep gradients and its ability to be sampled at the fast rate necessary to make high detailed surveying feasible. It might also be noted that the entire Elura grid was surveyed with the vehicleborne system in one day representing an enormous cost saving over the figure published by Gidley and Stuart (1980) for proton precession surveying. The relative costs were \$ 1500/km for a proton precession survey and \$ 30/km for vehicleborne caesium.

4.4 Conclusion

The effect of aliasing due to undersampling of a noise magnetic profile has been calculated theoretically and determined experimentally. The experimental results show that with a sensor height of 0.5 metre and a sample interval of 0.25 metre, there is insignificant noise energy in the signal frequency range. Increasing the sample interval, however, introduced aliased energy into signal band and provided a source of noise which could not be filtered without prior knowledge of the shape of the signal spectrum.